

A quantum mechanical view of molecular alignment and cooling in seeded supersonic expansions

V. Aquilanti, D. Ascenzi, M. de Castro Víttores,^{a)} and F. Pirani^{b)}
Dipartimento di Chimica dell'Università, 06123 Perugia, Italy

D. Cappelletti
Istituto per le Tecnologie Chimiche dell'Università, 06125 Perugia, Italy

(Received 26 March 1999; accepted 10 May 1999)

Experimental investigations on the collisional alignment of the rotational angular momentum, occurring in supersonic seeded beams and in drift tubes, have recently documented a strong dependence of the observed effects on the final molecular velocity. The present investigation aims at elucidating the possible mechanisms at the molecular collision level. Quantum state-to-state differential scattering cross sections, calculated for the prototype system O₂-He, for an interaction potential previously obtained in this laboratory, exhibit propensities relevant to reveal nature and selective role of the elastic and inelastic scattering events, participating in the overall mechanisms which lead to molecular alignment and cooling. The present analysis shows that the dynamics of such phenomena crucially depends on the initial and final rotational state, on the collision energy, on the involved orbital angular momentum and therefore alternative routes are possible for molecular polarization and relaxation. These routes lead to scattering into specific angular cones and therefore observations from different experiments provide complementary pieces of information which, exploiting studies of various molecular systems under diverse experimental conditions, can be correlated in a single mosaic. © 1999 American Institute of Physics. [S0021-9606(99)01729-8]

I. INTRODUCTION

A natural source of aligned and internally cold molecules involves the use of molecular beams "seeded" with lighter carrier gases: collisions occurring during the supersonic expansion produce molecules in low roto-vibrational states with specific alignment of the rotational angular momentum. This paper reports a quantum-mechanical study of atom-molecule collisions of relevance to the interpretation of recent experimental developments, including the discovery of the dependence of the alignment on the final molecular speed.¹

An early qualitative discussion was advanced by Gorter in 1938² to account for thermal conductivity experiments on flows of oxygen molecules.³ According to the Gorter mechanism, molecules flying with the rotational angular momentum perpendicular to the flow direction (*edge-on* configuration) offer a smaller target to collisions and thus suffer less randomizing events than those traveling *broad-side*, i.e., with the rotational angular momentum parallel to the flow direction. The net result would be a prevalent *edge-on* alignment of the molecules in a flow system. Later, Ramsey⁴ proposed the possibility of aligning angular momenta of molecules and open-shell atoms by collisions in molecular beams, by exploiting the selective attenuation through a buffer gas and sampling the beam of transmitted species.

Molecular alignment is now recognized as a prominent phenomenon occurring in supersonic gaseous expansion as

the result of a myriad of molecular collisions. After the first experimental observation by Steinfeld and Korving (as reported in Ref. 5), earlier evidence for collisional alignment in molecular beams was limited to some rotational states of alkali dimers.⁵⁻⁸

The potential interest of aligned molecules for collision dynamics studies has also long been recognized.⁹ Accordingly, considerable efforts have been dedicated¹⁰⁻¹⁸ to produce and probe collisional molecular alignment for a variety of species beyond the early "alkali age." Large attention has been devoted to characterize its dependence on parameters such as source pressure, nozzle shape, rotational state, angular displacement from the beam axis,¹⁰⁻¹⁵ and recently, the final molecular velocity.^{1,16-18} The observed features were found to be often incompatible with the Gorter mechanism and difficult to unify in a homogeneous description, even for systems expected to behave similarly.¹⁹ Indeed the complete characterization of this complex phenomenon to a microscopic level is of basic importance to properly plan a great variety of experiments with supersonic seeded beams of diatomic or polyatomic molecules of different type, as well as of open shell species.

An important application of molecular beams with controlled rotational alignment is the study of the anisotropy of intermolecular forces. Scattering cross sections of aligned O₂ molecules on Kr and Xe²⁰ and on O₂²¹ have been measured and their analysis, based upon close-coupling quantum mechanical calculations, has provided an accurate characterization of the interactions at intermediate and large intermolecular distances.

Our recent progress on the understanding of the colli-

^{a)}Present address: Unidad de Láseres y Haces Moleculares, Universidad Complutense de Madrid, 28040 Madrid, Spain.

^{b)}Electronic mail: pirani@dyn.unipg.it

sional alignment phenomenon is discussed in this paper by presenting extensive numerical calculations based on exact solutions of the quantum mechanical atom-diatom scattering problem. Section II provides the proper background by analyzing the relevant experimental information and illustrating the models which are available for their interpretation. Exact and approximate methods employed to describe scattering events are summarized in Sec. III and propensities emerging from the calculated quantum scattering cross sections are outlined in Sec. IV. A discussion of possible alignment mechanisms, useful to unify in a single picture the experimental information coming from different sources, is presented in Sec. V. Discussion and conclusions follow in Sec. VI. An Appendix reports a discussion of the role of angular momentum coupling (particularly of spin) in the case of O₂.

II. EXPERIMENTAL BACKGROUND AND EARLY MODELS

The collisional alignment of molecules in a nozzle expansion under supersonic conditions was first noticed for I₂ by Steinfeld and Korving,⁵ by means of a laser induced fluorescence technique. In 1974 Sinha, Caldwell, and Zare⁵ found, with an analogous technique, a significant alignment of Na₂ in supersonic beams of sodium atoms containing dimers, and later similar prominent effects were observed for other alkali-metal dimers.⁶⁻⁸ The search for other suitable molecular candidates required longer times: for I₂ another early report suggested a small alignment⁶ and a later one an appreciable effect.⁹ Qualitative evidence of a prominent effect were reported later¹⁰ for CO in the first excited rotational level and for the molecular ion N₂⁺ (in the rotational levels 4 and 10) drifted in He.¹¹ Pullman, Friedrich, and Herschbach,¹² probing the beam well downstream from the source, investigated supersonic expansions demonstrating the alignment to be facile and large by seeding I₂ molecules with various gas carriers. The lightest carrier gas H₂ was found to foster the largest alignment, followed by He and by the other heavier rare gases.

In all of the preceding studies, molecules flying *edge-on* have been found to predominate: this finding was confirmed for iodine¹² but increasing the source pressure, the sign of rotational alignment was found to be reversed, favoring *broad-side* configurations. The onset of the reversal depended strongly on the rotational state probed (see also a previous report on Na₂.⁶)

Collisional alignment was reported also for thermal N₂ expanded from a multichannel array¹³ and a dependence of the effect on the lateral displacement from the center of an iodine jet was noticed.¹⁴

More recently an extensive investigation in a jet expansion has been carried out for CO₂,¹⁵ confirming the general features but also showing some aspects in disagreement with previous findings. In particular H₂ was found to lead to a smaller degree of alignment than the one observed for He and no evidence of the reversed alignment mechanism, reported for I₂,¹² was noticed for CO₂, even at the largest source pressure values.

All of the studies reported so far witness the marked influence of nozzle geometry and source pressure on the

alignment degree, suggesting that competitive microscopic mechanisms may concur to the process of collisional alignment. Differences in the experimental findings appear when molecules with very different moment of inertia and bond lengths (i.e., I₂, Na₂, CO₂) are involved. Crucial are also the differences in experimental conditions, for example for measurements carried out either near the nozzle¹⁵ or well downstream with highly collimated beams¹² (i.e., with very different sampling angular cones).

In 1994 we presented the first evidence for a strong dependence of rotational alignment on the final speed, for oxygen molecules emerging from supersonic expansions,¹ by measuring the variation of paramagnetism in continuous seeded beams. The O₂ molecule has an open-shell configuration and the electronic spin **S** (responsible for its magnetism) and the nuclear rotation **K** angular momenta are coupled to give the total angular momentum **J**. During the collision process **K** and **S** are decoupled (see the Appendix), and any alignment of **K** gives rise to a nonstatistical distributions in the *J* components.²⁴

Subsequently, measurements of anisotropy effects²⁵ on collision cross sections for the O₂-Xe system, showed a marked dependence of these effects on the velocity of oxygen molecules within the same supersonic velocity distribution, and confirmed the correlation between molecular alignment and speed. This technique of probing alignment by scattering avoids problems regarding the knowledge of the behavior of the spin which, during the collisions, is effectively decoupled from **K** (see the Appendix).

Further scattering experiments, performed by using supersonic seeded beams of nitrogen molecules and exploiting anisotropy effects in the measured cross sections, yielded information on the rotational alignment for the case of N₂ and therefore in absence of electronic spin.²⁶ Comparison of the anisotropy effects measured in the scattering experiments of O₂ and N₂ carried out under similar supersonic seeded expansion conditions, provided further support for the degree of alignment obtained from the paramagnetism measurements.

After our initial reports on this subject,^{1,16} related works using laser probing of N₂⁺ drifted in He¹⁷ and of CO in a He seeded supersonic pulsed beam¹⁸ appeared, bringing further evidence of the dramatic dependence of molecular alignment on the final velocity. In^{1,16} it was shown that O₂ molecules in their rotational ground state *K*=1 were not significantly aligned at low velocities **v**, while the population of those flying *edge-on* (i.e., with **K**⊥**v**) was found to increase with the molecular speed²⁷ over those flying *broad-side* (**K**∥**v**). A qualitatively similar correlation between the degree of alignment and final velocity has been found for N₂⁺ (*K*=15) ions, drifted in He:¹⁷ for lower rotational states the alignment reverses its sign across the velocity profile. In the case of CO (*J*=6),¹⁸ (for this spinless molecule *J* is also the rotational quantum number) molecules with **J**⊥**v** were found dominant at the lower velocities while those flying *broad-side* (i.e., with **J**∥**v**) prevailed at intermediate velocities. The maximum polarizations found for O₂ and CO were about the same^{1,18} even if the velocity integrated alignment was lower for the CO case. For the *J*=4 state of CO the velocity distribution

of *broad-side* flying molecules was found similar to that for $J=6$, while the *edge-on* molecules were found accelerated and colder, resulting in a lower net polarization. Practically no alignment was found for the first excited rotational state ($J=1$).

The observed phenomenology is again expected to depend not only on the nature of investigated system, on the intermolecular potential, on the number and type of collisions promoting the alignment but also on the experimental set-up used. The purpose of the present study is to analyze in detail selectivity and role played by the microscopic scattering events leading to relaxation and alignment of the rotational angular momentum.

Several attempts have been performed in the past to model the mechanism of collisional alignment. The original Gorter mechanism,² based on simple hard-sphere cross section arguments, suggests that the observed prevalence of *edge-on* molecules is due both to their lower resistance to the flow, with respect to *broad-side* ones, and to the larger propensity of the latter to undergo randomizing collisions. The success of Gorter-like ideas along the years is based on their simple geometrical appeal, but such an approach is clearly inadequate to describe effects arising selectively from relaxation processes. The early experiments in molecular beams were discussed in terms of a ‘‘hard ellipsoid of revolution’’ model⁵ which does not distinguish between elastic or inelastic processes although some attention was devoted to the possible role of reactive exchanges. However, soon the hypothesis was formulated⁶ that the collisional alignment be determined by an anisotropic component in the scattering cross section, manifesting itself because of the ‘‘velocity-slip’’²⁸ between the carrier gas atoms and the seeded molecules.

According to a more recently proposed mechanism,¹² alignment depends on a balance of elastic and inelastic processes. This model, based on a competition between a ‘‘bulk’’ alignment mechanism due to elastic collisions (essentially the Gorter ideas) and an ‘‘anisotropic rotational cooling’’ mechanism, accounts for the fact that molecules in an *edge-on* configuration suffer both less randomizing collisions and more efficient rotational relaxation than those in a *broad-side* configuration. As a consequence, low rotational states, mainly formed by relaxation processes are expected to be preferentially aligned in the *edge-on* geometry while for molecules in high rotational states the effect of the depopulation originates an opposite behavior. Models based on classical trajectory calculations by the same authors²⁹ supported these ideas and, by comparing alignment found over a wide range of collision energies and impact parameters, pointed out three distinct regimes: for direct-mode collisions a ‘‘near-Gorter’’ and an ‘‘anti-Gorter’’ regimes were found for small and large impact parameters, respectively; a ‘‘pseudo-Gorter’’ behavior was also found and related to long lived complex formation. This study pointed out clearly the limits of the Gorter mechanism, suggesting the need of more accurate approaches to describe effects which may selectively depend on the impact parameter, as the velocity dependence of the alignment.

III. THE QUANTUM TREATMENT OF ATOM-DIATOM COLLISIONS

The theoretical treatment of the extreme collisional cooling and alignment which arise from internal-to-translational energy transfer and from the conversion of anisotropic velocity distributions into angular momentum polarizations requires a formulation where elastic and inelastic collisions are considered at a quantum level. Earlier approaches focussed mainly on velocity polarized rotational transfer cross sections, or state-multipole-tensor cross sections.^{30–35}

These quantities, related to state-to-state integral cross sections by recoupling transformations, imply partial wave summations and therefore carry no information on angular dependence of the scattering events. Complete quantum mechanical studies of atom-diatom collisions is currently within reach of presently available computational facilities.

The scattering amplitude for a transition between an initial and a final rotational state of a diatom (as a rigid rotor) was given by Arthurs and Dalgarno.³⁶ General expressions for state resolved integral cross sections in terms of basic inelastic T -matrix elements have been given by Reuss and Stolte³⁷ as well as by Alexander, Dagdigian, and DePristo for the collision frame³¹ and by Alexander and Davis for the laboratory fixed frame of reference.³³

The earlier formalism, which originates from methods developed to analyze experiments on the degree of fluorescence polarization from excited states and on pressure broadening of spectral lines, was also used by Mayer and Leone³⁸ to express anisotropic distributions of the rotational angular momentum induced by transport phenomena. Relationships between integral tensor cross sections and generalized transport cross sections have been given explicitly by Liu and Dickinson.³⁹

Follmeg, Rosmus, and Werner⁴⁰ studied the collisional induced alignment of N_2^+ ions drifting in a helium buffer gas by quantum close coupling calculation of the integral tensor cross sections and using an *ab initio* potential energy surface.⁴¹ The resulting collisional alignment was found to be smaller than the experimental value.¹¹ In addition, as also pointed out by the same authors in a subsequent work,⁴² a complete explanation of the observed alignment effects requires the knowledge of tensor cross sections over a wide range of collision energy, to take properly into account experimental averaging over the relative velocity distributions. Therefore, a full quantum mechanical analysis becomes cumbersome, because of extremely expensive computations of the necessary tensor cross sections. These problems stimulated the search of approximate methods, such as classical trajectories calculations, capable to replace close-coupled approaches to analyze experimental observable. To this purpose a comparison has been presented⁴² between calculations of inelastic state resolved and integral tensor cross sections, performed both with classical trajectories and close-coupled approaches and using the same *ab initio* potential energy surface. Results, which appear to agree only semiquantitatively, suggest that more marked differences can be expected in the state to state differential cross section, when calculated with classical and quantum methods.

Recent evidence on the velocity dependence of colli-

sional alignment (see Sec. II) requires a substantial modification of previous approach since the selective role of the different orbital angular momenta (classically of different impact parameters) must be taken into account. Therefore, to quantitatively describe these new alignment effects it is necessary to take into account state-to-state differential cross sections [(DCS) in the following]; as a consequence, both the previously outlined approach as well as simpler models based on classical mechanics are not adequate.

In this work extensive exact close-coupling quantum mechanical calculations of state-to-state differential cross sections have been carried out using an accurate interaction potential for the O₂-He system, previously obtained in this laboratory.⁴³ During each collision the rotational angular momentum \mathbf{K} of O₂ molecule is decoupled from the electronic spin \mathbf{S} (the minor role of spin on the scattering is discussed in the Appendix).

Although the formalism for close coupling calculations of state-to-state DCS has also been fully developed,^{31,33,44} no extensive investigations have been reported. Explicitly DCS for the scattering of a diatom by a closed shell atom is obtained as a weighted sum of contributions of partial cross sections each one corresponding to a particular value of the total angular momentum \mathcal{I} . The initial and final states of the diatom are labeled $|K_i M_i\rangle$ and $|K_f M_f\rangle$ respectively where M_i and M_f are the projections of \mathbf{K} along the initial relative velocity direction to be referred to as helicities in the following. The DCS can be calculated (see for example Refs. 31 and 44) as

$$\begin{aligned} & \frac{d\sigma_{K_i M_i, K_f M_f}}{d\Theta} \\ &= \left(\frac{\pi}{k_{K_i}^2} \right) \sum_{\mathcal{I}, l_i, l'_i, l_f, l'_f} (2\mathcal{I}+1) i^{l'_f - l'_i - l_i + l_i} \\ & \quad \times [(2l_i+1)(2l'_i+1)]^{1/2} \begin{pmatrix} K_i & l_i & \mathcal{I} \\ M_i & 0 & -M_i \end{pmatrix} \\ & \quad \times \begin{pmatrix} K_i & l'_i & \mathcal{I} \\ M_i & 0 & -M_i \end{pmatrix} \begin{pmatrix} K_f & l_f & \mathcal{I} \\ M_f & M_i - M_f & -M_i \end{pmatrix} \\ & \quad \times \begin{pmatrix} K_f & l'_f & \mathcal{I} \\ M_f & M_i - M_f & -M_i \end{pmatrix} T_{K_i, l_i, K_f, l'_f}^{\mathcal{I}} T_{K_i, l'_i, K_f, l'_f}^{\mathcal{I}*} \\ & \quad \times Y_{l'_f, M_i - M_f}^*(\Theta) Y_{l_f, M_i - M_f}(\Theta), \end{aligned} \quad (1)$$

where k_{K_i} is the wavenumber of the system in the entrance rotational channel K_i , the terms in brackets are $3j$ symbols and l_i and l_f , the orbital angular momentum quantum numbers, take all the allowed values; Θ denotes the center-of-mass (cm) scattering angle. The calculation of the scattering cross sections requires the use of extensive close-coupling, numerical techniques. We have used the MOLSCAT package⁴⁵ to calculate the T -matrix elements with proper modifications, in order to obtain the state-to-state DCS from Eq. (1) and to generate both excitation and relaxation cross sections.

Calculations have been performed in the CM frame at several collision energies, to cover the velocity-slip range

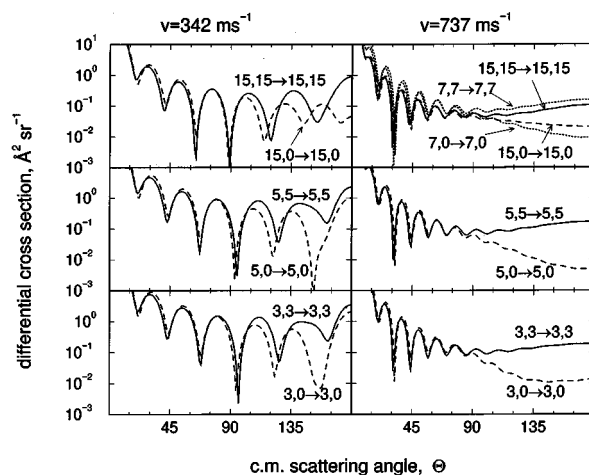


FIG. 1. Elastic cross sections with no helicity change: quantum mechanical state-to-state DCS, for the O₂-He system, calculated at two different relative collision velocities, $v=342 \text{ ms}^{-1}$ (left-hand column) and $v=737 \text{ ms}^{-1}$ (right-hand column), are plotted as a function of the center of mass scattering angle Θ . Results for elastic collisions with helicity conservation ($\Delta K=0$, $\Delta M=0$) of *edge-on* ($M=0$, dashed curves) and *broad-side* ($M=K$, continuous curves) molecules are reported for four different rotational states K . Numbers indicate initial and final K and M values.

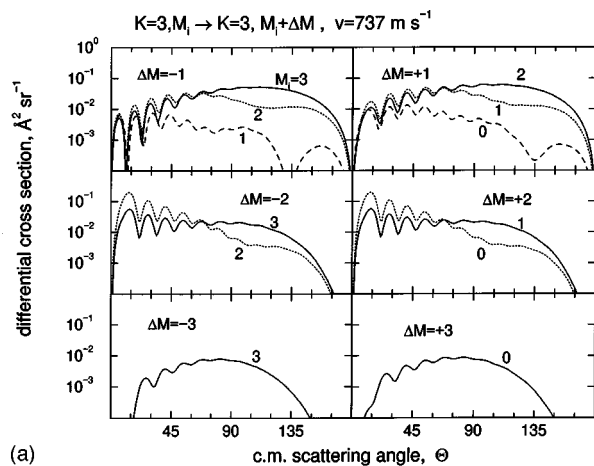
occurring in the experimental expansion of O₂ seeded in He, and considering various initial rotational states in order to account for the O₂ broad rotational distribution in the source.^{1,16} For the present system convergence required the coupling of all the open rotational channels as well as some of the first closed ones. The motivation of such extensive calculations must be found in the search of propensities and trends in the scattering from an anisotropic potential. Even if the alignment of molecules in a supersonic expansion is the result of many collisions the elucidation of systematic propensities in single collision events may shed light on the alignment mechanisms.

IV. RESULTS: PROPENSITIES IN THE STATE-TO-STATE DIFFERENTIAL CROSS SECTIONS

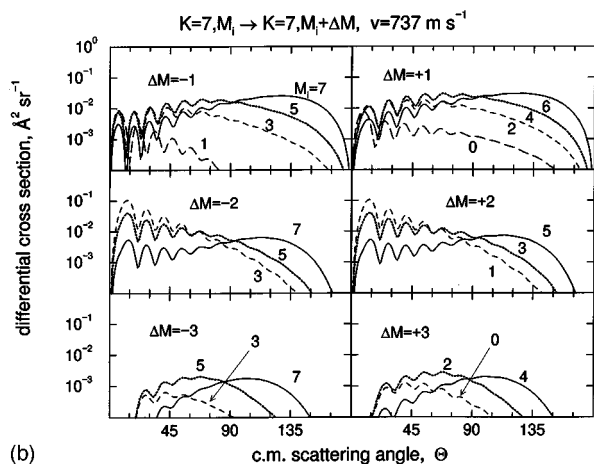
Extensive calculations have been carried out in order to characterize the dependence of the scattering features on the collision energy and on the initial and final rotational levels $|K_i M_i\rangle$ and $|K_f M_f\rangle$. In the following Fig. 1–6 only some representative results obtained will be shown for the cm frame and any dependence on other relevant quantities, when not explicitly shown in the figures will be discussed in the text.

State-to-state DCS can be classified as *elastic* (when the rotational quantum number K and helicity M are both conserved or when K is conserved but M varies) and *inelastic* (when K varies and M is conserved or when both K and M vary).

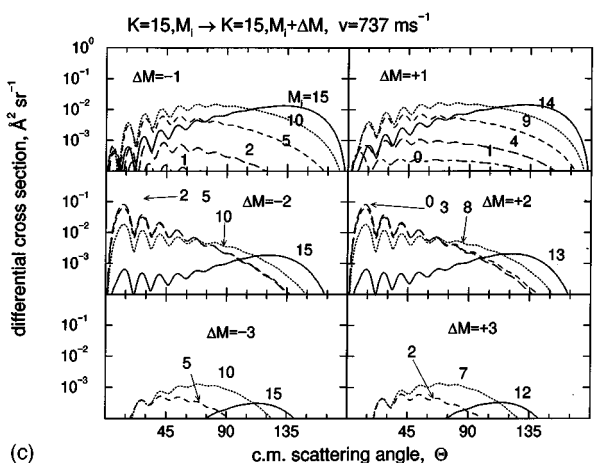
Figure 1 reports *elastic cross sections with no helicity change* for either $M=0$ or $M=K$. These two limiting values are the closest quantum-mechanical analogues of the classical *edge-on* and *broad-side* molecular configurations. Collisions at low orbital angular momentum (classically corresponding to small impact parameters b), leading to backward



(a)



(b)



(c)

FIG. 2. (a) Elastic cross sections with helicity variations: as in Fig. 1 and at the relative collision velocity of 737 m s^{-1} . Results for elastic collisions with helicity variation ($\Delta K=0, \Delta M=\pm 1, \pm 2, \pm 3$) are shown for $K=3$. Numbers indicate the initial helicity state M_i . (b) Elastic cross sections with helicity variations: as in Fig. 2(a) for $K=7$ and relative collision velocity of 737 m s^{-1} . Only selected examples of each set of ΔM data are shown. (c) Elastic cross sections with helicity variations: as in Fig. 2(a) for $K=15$ and relative collision velocity of 737 m s^{-1} . Only selected examples of each set of ΔM data are shown.

scattering at angles $\Theta \geq \pi/2$, exhibit a higher cross section for the *broad-side* approach. The difference attenuates as K increases and vanishes for forward scattering, involving collisions at high orbital angular momentum (classically, large

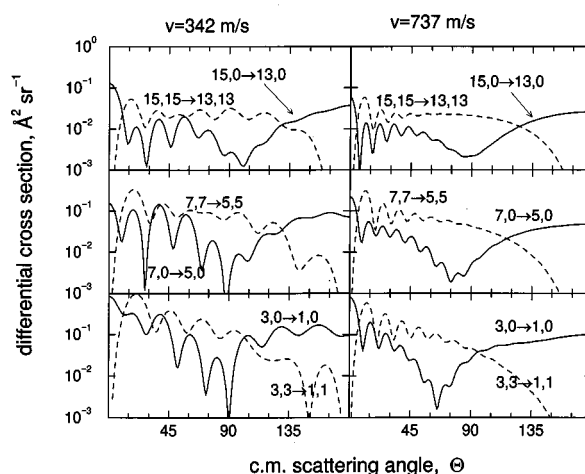
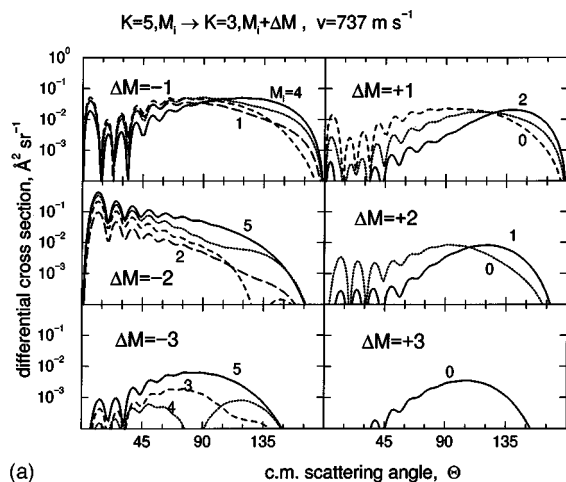


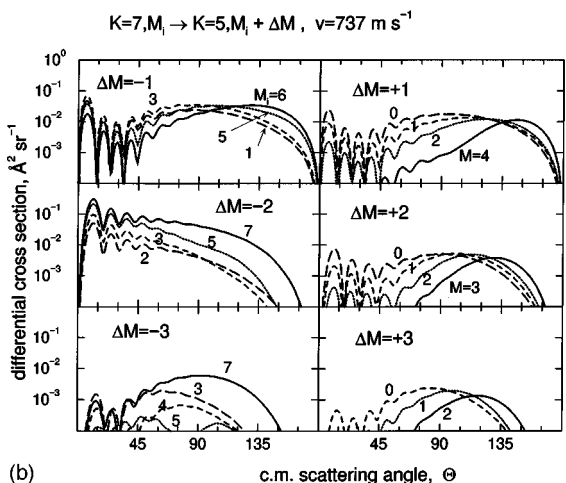
FIG. 3. Rotational relaxation cross sections for edge-on and broad-side molecules: as in Fig. 1, for two different relative collision velocities, $v = 342 \text{ m s}^{-1}$ (left-hand column) and $v = 737 \text{ m s}^{-1}$ (right-hand column). Results for inelastic collisions ($\Delta K = -2$) of *edge-on* (continuous curves) and *broad-side* (dashed curves) molecules in three different rotational states K are reported. Numbers indicate initial and final K and M states.

impact parameter b). Other results (not reported) suggest also an attenuation of such a difference for higher collision energies. This behavior, apparently in line with the Gorter mechanism, actually, from a quantum mechanical viewpoint, is seen to emerge from a more complex picture. First of all, a key role is played by both the repulsive and the attractive anisotropic components of the interaction, whose relative importance depends on the collision energy. Second, for *edge-on* molecules colliding at small impact parameters, both rotational excitation and relaxation (see later) are operative: they do not occur for the *broad-side* approach.

In Figs. 2(a)–2(c) are shown *elastic cross sections with helicity variations*. Nearly *broad-side* aligned molecules undergo helicity changes $M_f = M_i \pm 1$ particularly resulting from events with low orbital angular momentum (small b) leading to large scattering angles. Such contributions shift towards smaller scattering angles (collisions at larger b) and become negligible, as the initial helicity decreases. This result is consistent with the Gorter's suggestion that *broad-side* molecules are randomized more efficiently than *edge-on* ones. The $M_f = M_i \pm 2$ bending of nearly *broad-side* molecules is also operative in the large Θ range although not so large as for ± 1 changes. The occurrence of the same bendings of the rotational plane, corresponding to ± 1 and ± 2 helicity changes, for nearly *edge-on* encounters, is seen to shift towards smaller Θ (larger b), and ± 2 changes dominate over the ± 1 ones. This behavior can be ascribed to the increased and selective role of the centrifugal potential, which induces helicity changes through Coriolis coupling. Events with $M_f = M_i \pm 3$ have a much smaller probability, ending up mainly in the intermediate angular range. These features of M -changing cross sections do not vary significantly with the rotational state, although total cross sections, as obtained by integrating over the scattering angle Θ (not shown), decrease as K increases. Physically this corresponds to an increase of gyroscopic stability for faster rotors. Also, M -changing cross



(a)



(b)

FIG. 4. (a) Rotational relaxation cross sections with helicity change: as in Fig. 1 and at the relative collision velocity of 737 ms^{-1} . Results for inelastic collisions ($\Delta K = -2$) with helicity variations $\Delta M = \pm 1, \pm 2, \pm 3$ are shown, for the initial $K=5$ state. Numbers represent initial helicity state M_i . (b) Rotational relaxation cross sections with helicity change: as in Fig. 4(a) at the relative collision velocity of 737 ms^{-1} and for the initial $K=7$ state. Only selected examples of each set of ΔM data are shown.

sections depend very slightly on the collision energy, therefore the role of M -changing collisions is emphasized at higher energies where the elastic components with helicity conservation becomes significantly smaller. This is another manifestation of the increasing role of the Coriolis coupling.

Figure 3 presents rotational relaxation cross sections for *edge-on* and *broad-side* molecules. Only the dominant relaxation channels (those with $K_f = K_i - 2$) are shown (see Fig. 6 for other cases). In general, it can be noted that *edge-on* molecules can cool down to a lower K state without helicity variation, while *broad-side* ones require also a decrease of the helicity in order to rotationally relax. Present results suggest that relaxation with helicity changes are not allowed for scattering angles close to the CM backward direction. An appreciable centrifugal potential must be operative in order to induce bending of the rotational plane through Coriolis coupling (see also Fig. 2). Therefore, the relaxation of *edge-on* molecules can be significantly induced by collisions also at low orbital angular momentum (classically, small impact parameter b), leading to backward scattering. The cor-

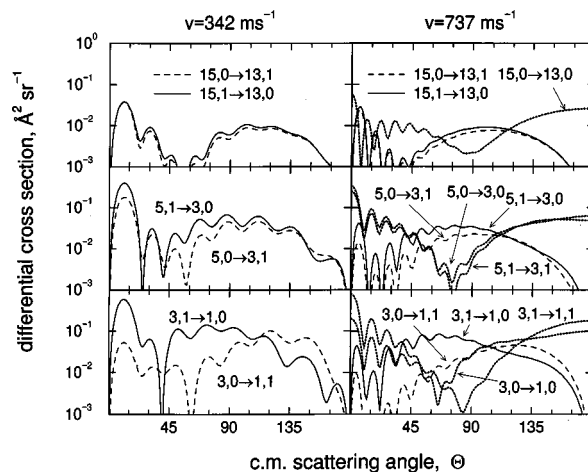


FIG. 5. Rotational relaxation cross sections of molecule in low helicity states: as in Fig. 1, for two different relative collision velocities, $v = 342 \text{ ms}^{-1}$ (left-hand column) and $v = 737 \text{ ms}^{-1}$ (right-hand column) and refer to the inelastic collisions ($\Delta K = -2$) of near *edge-on* (low helicities) molecules in three different initial rotational states $K = 15, 5$ and 3 . Number represent initial and final K, M states. Continuous curves indicate processes with $\Delta M = -1$, dashed curves $\Delta M = +1$ and dotted curves $\Delta M = 0$ respectively.

responding cross sections are comparable with (and often larger than) the elastic ones of Fig. 1. In turn, *broad-side* encounters exhibit higher probability to give rotational relaxation in the small Θ (large b) range, where the inelastic cross sections are lower or comparable with the elastic ones of Fig. 1. These features are common to all the collision energies and rotational states studied, and suggest that the relaxation in the backward direction of *edge-on* molecules is an effective process during the whole evolution of the supersonic expansion, although at the earlier stages it is competitive with rotational excitation. Since *broad-side* molecules require a helicity decrease in order to rotationally relax, for them such a process occurs at larger orbital angular momenta and leads to scattering at smaller Θ . On the whole it appears from Fig. 3 that the efficiency of rotational relaxation increases with the decrease of the rotational state K .

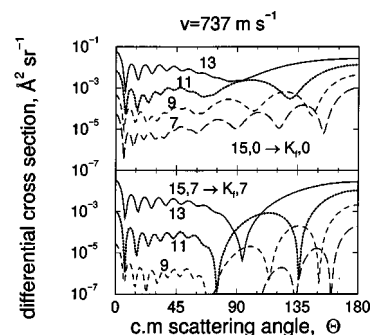


FIG. 6. Relaxation cross sections with large K variations and helicity conservation: as in Fig. 1, for the relative collision velocity of 737 ms^{-1} . Results for inelastic collisions with $\Delta M = 0$ and $\Delta K = -2, -4, -6$ and -8 , are reported for comparison for the initial $K=15$ rotational state. The upper panel refers to the $M_i = M_f = 0$ cases while the lower one refers to the $M_i = M_f = 7$ cases. Numbers represent final K states.

Figures 4(a) and 4(b) show *rotational relaxation cross sections with helicity change* for initial rotational states $K_i = 5$ and $K_i = 7$, respectively. Examples reported refer to the $K_f = K_i - 2$ processes and illustrate the behavior of collisions with ± 1 , ± 2 , and ± 3 helicity variations. General trends are similar to those for elastic collisions with helicity variations of Fig. 2, but there are also some important differences. In particular, relaxation cross sections with a decrease of the helicity are significantly larger than the corresponding ones with an increase of the helicity. This effect is particularly evident for the ± 2 process, leading to intermediate and small scattering angles. Other features to be contrasted with those of Fig. 2 include the behavior of relaxation with helicity variation from 1 to 0, here an important process at intermediate scattering angles, and of the $M_f = M_i - 2$ collisions of *broad-side* molecules, whose cross sections are here more effective at small scattering angle (see also Fig. 3). Results in Figs. 4(a) and 4(b), and others not shown, indicate that all these relaxation processes appear to decrease for higher initial rotational states (see also Fig. 3).

Rotational relaxation cross sections ($K_f = K_i - 2$) of molecules in low helicity states are compared in Fig. 5. The $M_f = M_i$ components present a near forward-backward symmetry with a sideways "window," where the onset of $M_f = M_i \pm 1$ processes occurs. Three main features must be pointed out: (i) within the window, the $1 \rightarrow 0$ helicity change component is always higher with respect to the $0 \rightarrow 1$ one; (ii) the difference between the competitive $1 \rightarrow 0$ and $1 \rightarrow 1$ channels is larger than the difference between the corresponding (and competitive) $0 \rightarrow 1$ and $0 \rightarrow 0$ ones; and (iii) all these effects are more pronounced as the rotational state decreases.

Relaxation cross sections with large K variations and helicity conservation are compared in Fig. 6. Calculations are presented for the initial $K_i = 15$ state and for two different helicities. The $K_f = K_i - 2$ processes, as expected, appear to be the dominant relaxation channels and indeed the cross sections regularly decrease with the increase of the inelasticity. This result suggests that for the present system the overall relaxation phenomenon in the supersonic expansion is mainly governed by a sequence of $K_f = K_i - 2$ inelastic events.

V. ALIGNMENT MECHANISMS IN A SUPERSONIC EXPANSION

The phenomenology illustrated in the previous section shows propensities and suggests a scenario of mechanisms whose relative roles are expected to change for different molecules and experimental conditions.

Three regions can be identified as a supersonic seeded expansion evolves in the forward direction along the expansion axis:¹⁴ first, a *continuous-flow region*, where the velocity slip between seeded molecules and carrier gas atoms is largest,²⁸ characterized by a large number of elastic collisions as well as by competitive excitation and relaxation processes. In this region a net acceleration of the seeded molecules is due to momentum transfer by elastic events. In the *transition region*, elastic events still occur but the relative velocity is too small to induce rotational excitation: here re-

laxation becomes the dominant inelastic process, producing cooling and a further acceleration. When the molecular density becomes sufficiently low, the beam enters the last, *collision-free region*. The relative importance of the first two regions depends very much on the features of the investigated molecule-carrier gas system (masses, intermolecular potential, density of molecular rotational states,...).

In the *continuous-flow region*, the angular dependence of the processes is strongly washed out by the large number of collisions which cover the whole range of impact parameters and whose principal effects are acceleration and focusing of molecules in the forward direction in the laboratory (LAB) system.⁴⁶ A quantitative description of the dynamics in the *continuous-flow* region is very difficult and our discussion will be necessarily qualitative. In this region, the main source of alignment comes from elastic processes with helicity variations (see Fig. 2 as discussed in the preceding section): their importance is comparable with that of helicity conserving elastic events of Fig. 1, when the relative velocity is sufficiently high.²⁸ As also shown in the cartoon of Fig. 7, with respect to *edge-on* molecules, *broad-side* ones show a larger propensity to bend the rotational plane (see Fig. 2) and this provides the explanation at a microscopic level of the general observation that alignment occurs preferentially in favor of the *edge-on* configuration (Gorter-type mechanism). The final outcome depends on the total number of collisions and this mechanism also explains the general increase of the alignment with the $P_0 d$ parameter (P_0 is the gas pressure in the source and d is the nozzle diameter) at least for low P_0 values, that is when the relaxation is not extensive.^{12,15,16}

An important feature is the K dependence: molecules in high K states are less likely to bend than those in low K (see Fig. 2). On the other hand low K states are more easily depolarized by inelastic events (see Figs. 3–5; when open, excitation events behave similarly to relaxation). The net result may be an alignment that increases with the rotational state at least for the lowest rotational levels. This can be the case for a beam of alkali dimers for which rotational relaxation does not appear to be important (see for instance Ref. 7).

A limited number of molecules which have experienced collisions at low orbital angular momenta (classically, at small impact parameters b) remain in the *broad-side* configuration (see Fig. 1). In this stage of the expansion, these molecules are expected to be slightly more accelerated by momentum transfer (see Fig. 7) than those following other routes.

In the *transition region*, corresponding to a lower molecular density, it is expected that a memory be maintained of the angular dependence of single scattering events. Since the relative collision velocity between carrier and seeded molecules (the velocity slip)²⁸ becomes smaller, the relaxation processes are competitive with (or even dominant over) the elastic events (see Fig. 3), at least for particular b ranges and for specific molecular orientations. Elastic collisions are still present but, because of the small momentum transferred, they are expected not to contribute much to the further acceleration of the molecules, mainly due in this region to rotational-to-translational energy transfer. Several mechanisms may concur to distinct angular distributions. Their

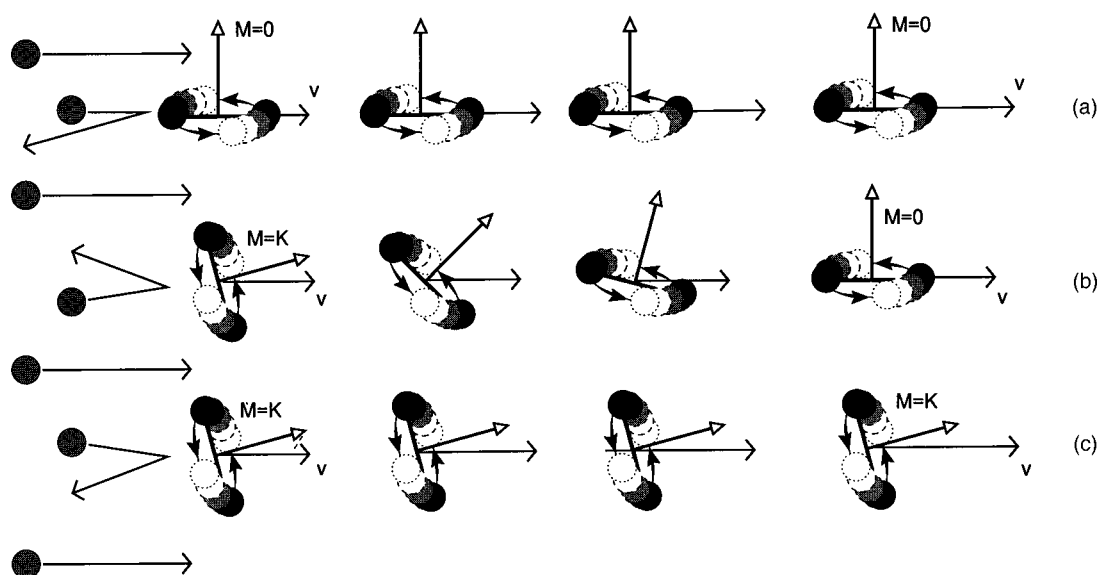


FIG. 7. Acceleration of molecules by elastic collisions with faster carrier atoms; (a) refers to *edge-on* encounters which maintain the helicity state; (b) and (c) describe the acceleration of *broad-side* molecules respectively with and without bending of the initial rotational plane.

relative importance depends also on the initial and final rotational states. This is consistent with the fact that the final rotational temperature in a supersonic expansion is lowest near the beam axis and increases moving towards the edges, as a consequence not only of the variation in the number of collisions but also of their nature. Therefore, for the same system the measured alignment may vary with the angular range of the expansion cone which a given experimental configuration probes. To shed light on the possible operative mechanisms it is necessary to take into account both the K distribution in the source and the internal energy available during the relaxation process. Figure 8 serves to visualize typical initial conditions of O_2 in our experiments. The oxygen molecules in the beam source, maintained at room temperature show a distribution of rotational levels with a broad maximum at levels $K=5$ and 7 and significant population up to $K=21$. In the present discussion, which amplifies a previous outline of our view of the phenomenon,^{1,16,19,47} we will distinguish three regimes of initial rotational states: high ($K \geq 15$), medium ($7 \leq K \leq 13$) and low ($K \leq 5$, see the upper panel of Fig. 8). We will further group the molecules according to *low* and *high helicity*.⁴⁸ Collisional events will be also divided, according to the involved range of orbital angular momentum (classically, the impact parameter b), into *small b* collisions (leading to backward CM scattering, $\Theta \geq \pi/2$) and *large b* collisions (leading to forward scattering, $\Theta \leq \pi/2$).⁴⁹

A. The high K regime

Low helicity molecules⁴⁸ can relax for *small b* collisions⁴⁹ (see Sec. IV and Fig. 3), maintaining or decreasing the initial *low helicity* (Sec. V and Figs. 3 and 5). These *edge-on* flying molecules (most of which will eventually be in the ground $K=1$ rotational state) are scattered in a Θ -range close to 180° (backward direction) in the CM sys-

tem, and so in the LAB frame are confined in a narrow cone in the forward direction around the beam axis. They also benefit of the largest forward acceleration coming from inelastic events (rotational-to-translational energy transfer). This mechanism is schematized in the upper cartoon reported in Fig. 9. Also shown is the Newton diagram for such a *small b* collision, demonstrating that only a small fraction of the available energy is transferred to the heavier oxygen in collisions with helium. However, since here relaxation starts from high K , many inelastic transitions are experienced by

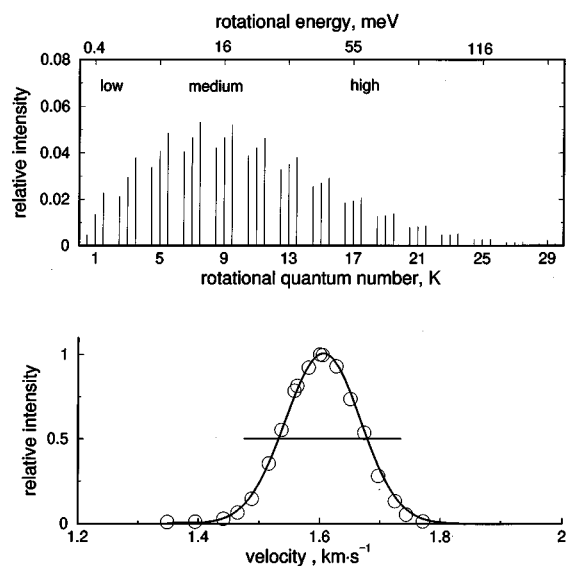


FIG. 8. Upper panel: distribution of the spin-rotational levels of O_2 in the beam source at room temperature. The rotational states are classified in three classes. The abscissa axis represent also a scale of the rotational energy corresponding to each K state. Lower panel: open circles describes the measured velocity distribution of an O_2 supersonic beam seeded in He, at a source pressure of 800 Torr. The line parallel to the abscissa axis defines the typical velocity increase of O_2 when it relaxes from a high K to the ground rotational level, because of inelastic collisions at short impact parameters.

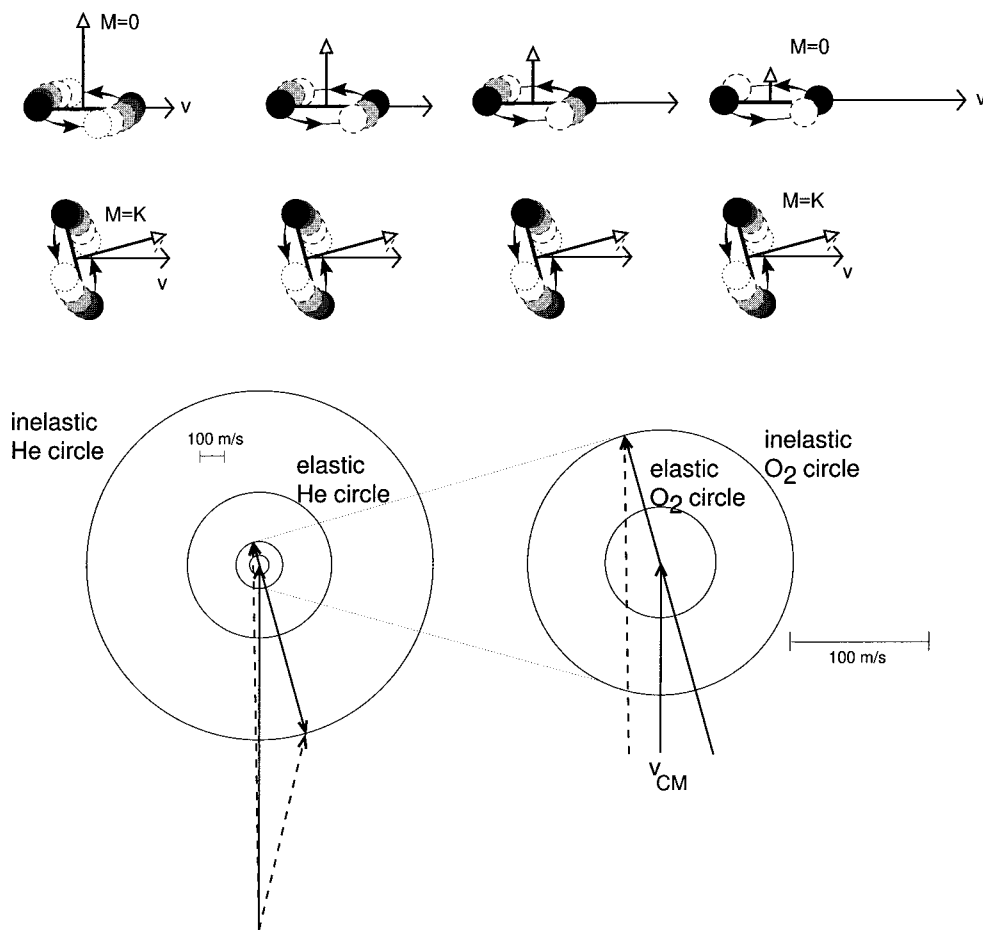


FIG. 9. The behavior of *edge-on* molecules which, when colliding at short impact parameters, can accelerate and relax because of inelastic events, is compared with the one of *broad-side* targets, which, when do not relax, continue to be accelerated only by elastic collisions. Molecules are backward-scattered in the CM frame which correspond to a forward LAB direction. Typical kinematic conditions for a collisions at $v=342\text{ m s}^{-1}$ are shown in the Newton diagram. The elastic and inelastic ($K=15\rightarrow 13$) circles are also reported and magnified in the right-hand side for the O_2 case, where the different acceleration due to inelastic and elastic events appears evident.

those molecules so that they eventually acquire an effective acceleration. To illustrate more quantitatively this effect we have reported in the lower panel of Fig. 8, a typical velocity distribution of O_2 seeded in He together with an estimate of the maximum velocity increase experienced by O_2 (forward scattered in the LAB frame), starting from an initial $K=21$ state, and reaching $K=1$. Such velocity variation is reported as a horizontal continuous line across the velocity distribution, centered on the maximum. It can be seen that such contribution can even be larger than the full width at half maximum of the distribution.

High helicity targets⁴⁸ for $b\sim 0$ suffer exclusively elastic collisions (see the lower cartoon in Figs. 9 and 3). These near *broad-side* flying molecules, confined in a narrow angular cone, are among the few remaining in the initial K level and are accelerated by elastic collisions both in the first and second region of the expansion. For nonzero (but *small b* collisions),⁴⁹ these molecules can bend and/or rotationally relax with and without helicity variation. We distinguish the following situations: (i) a small helicity variation, permits only a partial relaxation and therefore in practice a conservation of the original configuration; (ii) large helicity variation at the beginning of the process, which require multiple collisions permitting again only a partial relaxation but allowing bending towards *edge-on* configurations [this process is less favorable than the (i)]; (iii) the third possibility is rotational relaxation with a helicity decrease: this is the route that eventually leads to the ground rotational state. Such

molecules are expected to be less accelerated, less aligned and distributed in a wider angular cone with respect to those exhibiting originally *low helicity* and whose relaxation has been discussed earlier.

For *low helicity*⁴⁸ and *large b* collisions,⁴⁹ molecular scattering occurs at small Θ [Figs. 1, 2(c), 3, and 4], leading to an appreciable angular spread in the LAB (see Newton diagram in Fig. 10). Therefore, the relaxation process may be incomplete and leads only partially to the ground state. Since here the elastic cross sections with helicity variation [Fig. 2(c)] are larger than the inelastic ones (Figs. 3 and 4) and comparable with the helicity conserving elastic ones (Fig. 1), in this angular range *edge-on* molecules bend more easily. This implies that molecules relaxed in $K=1$ may not be aligned in the *edge-on* configuration. This behavior is illustrated in the cartoon of Fig. 10.

*High helicity*⁴⁸ molecules relax for collisions at *large b*,⁴⁹ mainly via a decrease of the helicity ($M_f=M_i-2$), and therefore their permanence in the initial rotational state is unlikely. Such inelastic channels show a cross section comparable (see Fig. 3) with the helicity conserving elastic components (see Fig. 1), while elastic processes with helicity variation [Fig. 2(c)], that we have seen to be important for other mechanisms, play here a minor role [they will have some effect only for small K , see Figs. 2(a) and 2(b)]. As for the previous route, molecules are only slightly accelerated and distributed in a wide angular cone with a probable leak of the initial alignment as K decreases (see Fig. 10).

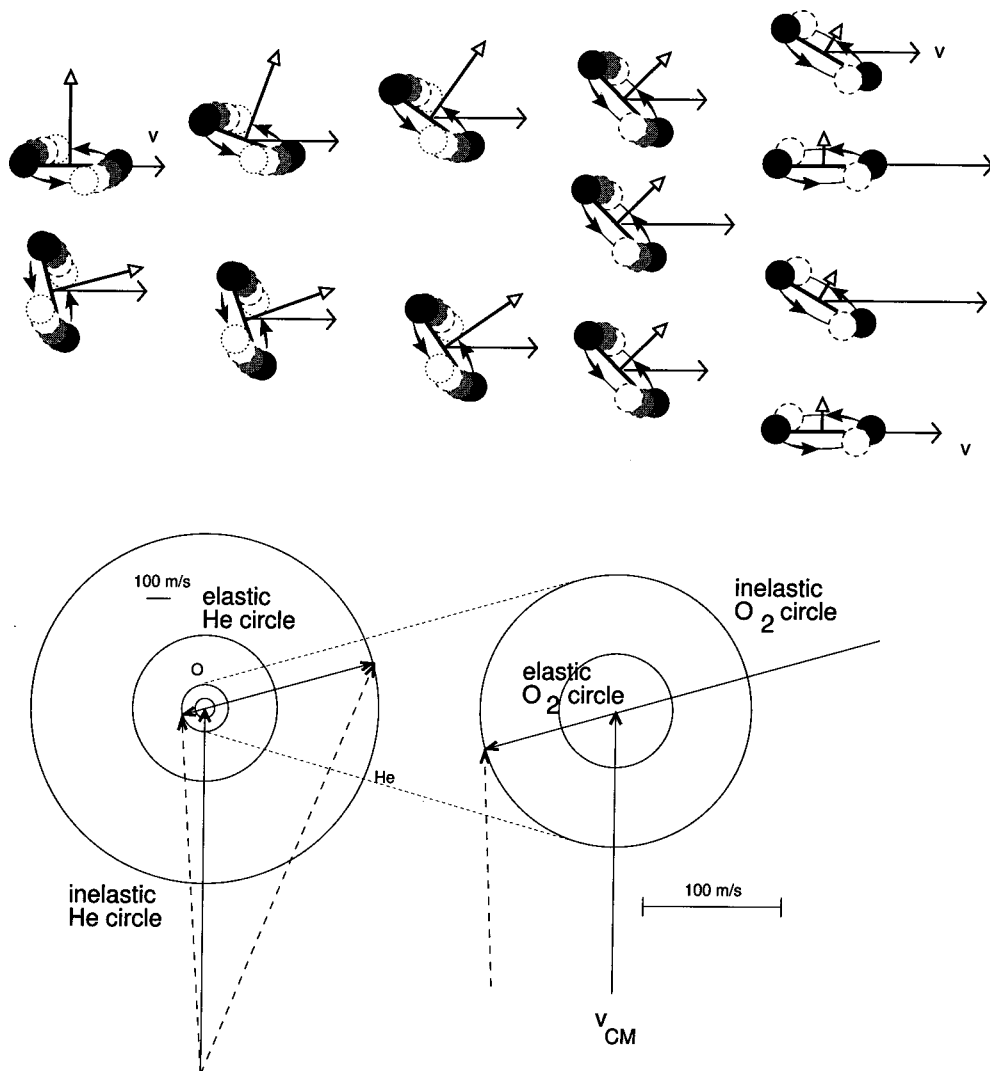


FIG. 10. The behavior of *edge-on* and *broad-side* molecules colliding at large impact parameters. The Newton diagram reported in the lower panel describes the same kinematics conditions as in Fig. 9 but here refers to a sideways scattering. It clearly indicates that molecules are less accelerated, less aligned, and distributed in a final wider cone (in the LAB system) than those in Fig. 9.

B. Intermediate K regime

The routes leading to relaxation are basically the same as discussed in the previous high K regime, although now the depolarization induced by rotational excitation can be more effective in the expansion. In addition, the role of some of the propensities should be less pronounced because of the occurrence of a reduced number of relaxation jumps.

Collisions at *small* b of *low helicity* molecules lead exclusively to the formation of the ground rotational state. As anticipated before, propensity to maintain or to further reduce the helicity state is less effective than for higher K , but still operative. Molecules are expected to be scattered in a small angular cone, as for higher K , although less accelerated and less aligned.

Collisions of *high helicity* molecules at *small* b mostly lead to the formation of the ground rotational state, although some of them can remain in the initial helicity and rotational states. These are those elastically scattered backward in the CM frame (Fig. 3) and in the LAB confined in a narrow cone in the forward direction (Fig. 9). Since in this case the transferred momentum is due exclusively to elastic collisions, the acceleration must be similar to that of the corresponding case

described for higher K . For nonzero b , elastic collisions with helicity variation and inelastic collisions with helicity decreasing become relevant, scattered molecules partially lose their initial alignment and are expected to be less accelerated and distributed in a larger angular cone than that of *low helicity* molecules (see earlier).

The relaxation to the ground rotational state of *low helicity* molecules colliding at *large* b is more complete for intermediate K than for high ones. Such collisions neither maintain nor induce alignment. They produce a modest acceleration and scattering in an angular cone larger than for *small* b collisions but lower than for the corresponding situation for higher K .

High helicity molecules can fully relax to the ground rotational state through inelastic collisions at *large* b involving helicity decreasing (see also the high K regime and Fig. 4). Molecules in the final ground rotational state have partially lost their initial alignment and are scattered in a larger cone than in the *small* b cases but smaller than for the corresponding situation of the high K regime, essentially because of the lower rotational energy available for conversion into translation.

C. Small K regime

Almost all molecules reach the ground rotational state independently from the involved range of orbital angular momentum (or impact parameter b). Selectivities and propensities in the rotational relaxation play here only a minor role. Also, mechanisms of elastic alignment are less effective. Scattered molecules are expected to end up in the tail of the final velocity distribution since accelerated exclusively by elastic collisions leading to negligible alignment.

VI. DISCUSSION

The calculations presented in Sec. IV and the relaxation mechanisms identified in Sec. V explain the relevant features of the collisional alignment experiments on O_2 molecules,^{1,16} particularly the velocity dependence of alignment in supersonic seeded expansions. Moreover, the present study can help us to fit into a unified picture other experiments on molecules with mass and rotational level spacings similar to O_2 , such as those on seeded CO expansion¹⁸ and drift-tube N_2^+ transport:¹⁷ they also show a considerable velocity dependence of the alignment, observed under different experimental conditions.

In the O_2 experiments,^{1,16} the continuous beams are analyzed well downstream, after ~ 1 meter from the nozzle orifice. The supersonic seeded beams are strongly collimated because of the presence of a first skimmer (1.2 mm in diameter) at ~ 1 cm from the nozzle, a second skimmer (1.2 mm in diameter) after ~ 10 cm and a final defining slit (0.7 mm in diameter) at about 1 m from the nozzle and before the probing region. The cone of acceptance is therefore $\leq 10^{-6}$ steradians. The coupling of the mechanical velocity selector inserted along the beam path with the unusually high angular resolution,¹⁶ allowed us to select molecules both in the longitudinal and in the transversal motion. Velocity on the latter is less than 1 m/s. Oxygen molecules sampled in these experiments are essentially those relaxed in the ground rotational state and traveling in a very narrow angular cone around the beam axis. Molecules emerging in such a cone are mainly those who have experienced elastic and inelastic collisions at small impact parameters (backward in the CM frame corresponding to LAB forward scattering) and only minor contributions come from those distributed in wider angular cones, as a result of more sideways (*large b*) collisions. From the discussion in Sec. IV of propensities in the scattering and in Sec. V on the alignment mechanisms, it appear that molecules analyzed in these experiments are mainly those coming from the relaxation processes at *small b*. Specifically, molecules traveling faster originate from relaxation mechanisms of high K states: their number is small but they are strongly aligned and accelerated by the large amount of rotational energy available for conversion into forward translational motion. Molecules originating from intermediate- K levels are those mainly contributing to the O_2 beam intensity: they travel at velocities close to the maximum of the distribution and exhibit an intermediate alignment. All the other channels lead to modestly aligned molecules with medium or low velocities.

The importance and selectivity of inelastic collisions are expected to decrease in experiments which probe not fully relaxed rotational states and which are carried out analyzing a much wider beam profile. In such cases a relevant role is again played both by elastic and inelastic contributions to the DCS, which now have to be properly integrated over the angular and velocity resolution functions of the experiments. These can lead to apparent differences in the observables (such as cooling and alignment), also in systems which may be expected to behave similarly in seeded supersonic expansions.

In Ref. 18, the 4th and 6th rotational states, which correspond to intermediate levels of the rotational distribution in the beam source, have been analyzed in the case of CO molecules in He seeded supersonic pulsed beams. From the velocity distributions probed near the nozzle (~ 6 cm) using a polarized laser light, it is found that slow velocity components of the molecular beam show a prevalence of *edge-on* geometries, whereas *broad-side* ones prevail for fast components. From the viewpoint suggested here, most of the *broad-side* molecules observed in these levels have flown maintaining the initial rotational state and helicity. They were accelerated exclusively by elastic collisions at *small b*, which conserve initial rotational and helicity states (Figs. 1, 3, and 9). Another appreciable contribution to the final states can also come from *broad-side* molecules initially in higher rotational levels, which undergo a small helicity variation and then can relax only partially maintaining the initial configuration. Similar arguments indicate that the formation of *edge-on* molecules in Ref. 18 can be ascribed as coming from an incomplete relaxation of higher levels, because of *large b* collisions mainly in the *edge-on* configuration. These molecules have a final smaller velocity having suffered elastic and inelastic collisions at *large b* with a low momentum transfer. This is consistent with Fig. 1 of Ref. 18, where *broad-side* molecules (which mainly suffered elastic scattering) show a similar velocity distribution for both rotational states 4 and 6, while *edge-on* molecules (more affected by inelastic scattering) are globally faster in state 4 than in state 6.

The experimental observation of an extremely small alignment degree for the first excited rotational state of CO, when contrasted with the marked alignment observed for O_2 in $K=1$,¹ must be due to the wide angular cone probed (see also Ref. 10).

The drift-tube experiments on N_2^+ ions^{11,17} show some important differences with seeded supersonic beams (where the velocity slip decreases along the expansion): the average relative collision speed is larger than the typical velocity slip and is kept constant by the applied electric field. Therefore in a drift tube the ions are aligned essentially by elastic mechanisms (see Secs. IV and V) and *edge-on* molecules are accelerated more effectively than *broad-side* ones since they offer the least resistance to the flow.

VII. CONCLUSIONS

The present analysis suggests that several molecular alignment mechanisms can be operative in a supersonic

seeded expansion, each one depending on the route followed by the molecule towards acceleration and cooling. The final state, i.e., speed, rotational level, type and degree of alignment, ..., depends on properties of the molecules as well as of the carrier gas (difference in mass, interaction potential anisotropy, density of the rotational levels, ...), on the number of collisions, the energetics and on the range of orbital angular momentum involved.

The quantum mechanical case studies presented here illustrate how the different collisional dynamics lead to molecules scattered into different angular cones in the LAB frame. The analysis of the experimental findings and any comparison among them must then properly take into account the observational details employed in their measurements and particular attention has to be devoted to the angular and velocity resolutions.

In conclusion, the present study which aimed at compacting in a unified picture several of the experimental observations on the rotational cooling and alignment of diatomic molecules in supersonic seeded beams (including the dependence on final speed) must be considered also as a starting point to understand the behavior of polyatomic linear or planar molecules.⁵⁰ It is also hoped that it will serve as a guide to plan and interpret collisional experiments with aligned molecules.

ACKNOWLEDGMENTS

This work is supported by the Italian National Research Council (CNR), by the Ministero dell'Università e della Ricerca Scientifica e Tecnologica (MURST), by the ENEA (Ente per le Nuove Tecnologie, l'Energia e l'Ambiente) and by the European Union through the programmes Training and Mobility of Researchers Network "Potential Energy Surfaces for Molecular Spectroscopy and Dynamics" [Contract No. ERB-FMRX-CT96-0088].

APPENDIX: ANGULAR MOMENTUM COUPLING IN COLLISIONS OF MOLECULAR OXYGEN

For collisions of molecular oxygen in the ground electronic state ${}^3\Sigma_g^-$ with a closed shell atom, the direction of the relative velocity \mathbf{v} is the proper quantization axis for the rotational angular momentum \mathbf{K} , its projection M correlating asymptotically with a collision helicity quantum number. Indeed \mathbf{K} and the electronic spin angular momentum \mathbf{S} are decoupled by the inhomogeneous electric field due to the forces which are driving the collision (i.e., at intermediate and short intermolecular distances the interaction potential and its anisotropy are always much larger than the spin-rotation coupling).

In a supersonic expansion, because of the high number of collisions experienced by each molecule with the faster carrier atoms, these electrostatic forces are those which are mainly responsible for cooling and alignment of the rotational angular momentum.

However, no guarantee can be given for \mathbf{v} being a good quantization axis either for \mathbf{S} decoupled from \mathbf{K} and for \mathbf{J} , especially for collisions involving low helicities. A natural quantization direction for the spin, which couples only

through a magnetic interaction, may rather be the direction of the orbital angular momentum of the colliding system, orthogonal with respect to the rotational plane of the van der Waals complex and therefore orthogonal to \mathbf{v} . This interaction, which depends on the anisotropy of the charge distribution in the collisional complex, on the impact parameter and on the orbital velocity, is expected to be much weaker than the electrostatic intermolecular potential and slowly varying with the intermolecular distance. A similar sequence of angular momentum coupling schemes is reminiscent of the Hund's (b) and (e) cases, describing rotational levels of diatomic molecules.

Therefore, the spin coupling in the collisional complex although not substantially affecting scattering processes, plays a relevant role in determining other properties of the van der Waals system. An interesting example of the role of the spin coupling is illustrated in Ref. 22.

To the present purpose it appears to be of more interest the recoupling of polarized \mathbf{K} with \mathbf{S} to give \mathbf{J} , which occurs between successive collisions in the expansion, leading to a natural depolarization effect.²³

The observation¹ of a strong increase of O_2 paramagnetism along the beam profile is the experimental manifestation that faster molecules travel in the *edge-on* configuration and exhibit also a polarization of the spin. Such polarization appears as a necessary condition to observe high alignment for $K=1$ far from the beam source.

At this stage it is difficult to quantitatively justify the observed effects: however, following suggestions given in Ref. 23, an alignment transfer can be hypothesized after the recoupling, from an aligned \mathbf{K} to an unpolarized \mathbf{S} . A high number of successive collisions are necessary to originate the observed effects (i.e., K alignment and spin polarization) and this indeed appears to be the case for a supersonic expansion.

¹V. Aquilanti, D. Ascenzi, D. Cappelletti, and F. Pirani, *Nature* (London) **371**, 399 (1994).

²C. J. Gorter, *Naturwissenschaften* **26**, 140 (1938).

³H. Senfleben, *Phys. Z.* **31**, 822 (1930). For further developments on the so-called Senfleben-Beenakker effect, see also J. J. M. Beenakker G. Scoles, H. F. P. Knaap, and R. M. Jonkman, *Phys. Lett.* **2**, 5 (1962); J. J. M. Beenakker and F. R. McCourt, *Annu. Rev. Phys. Chem.* **21**, 47 (1970).

⁴N. F. Ramsey, *Phys. Rev.* **98**, 1853 (1955).

⁵M. P. Sinha, C. D. Caldwell, and R. N. Zare, *J. Chem. Phys.* **61**, 491 (1974).

⁶A. G. Visser, J. P. Bekooy, L. K. van der Meij, C. de Vreugd, and J. Korving, *Chem. Phys.* **20**, 391 (1977).

⁷U. Hefter, G. Ziegler, A. Mattheus, A. Fischer, and K. Bergmann, *J. Chem. Phys.* **85**, 286 (1986).

⁸H. G. Rubahn and J. P. Toennies, *J. Chem. Phys.* **89**, 287 (1988).

⁹W. R. Sanders and J. B. Anderson, *J. Phys. Chem.* **88**, 4479 (1984).

¹⁰J. A. Barnes and T. E. Gough, *Chem. Phys. Lett.* **130**, 297 (1986).

¹¹R. A. Dressler, H. Meyer, and S. R. Leone, *J. Chem. Phys.* **87**, 6029 (1987).

¹²D. P. Pulmann, B. Friedrich, and D. R. Herschbach, *J. Chem. Phys.* **93**, 3224 (1990); B. Friedrich, D. P. Pulmann, and D. R. Herschbach, *J. Phys. Chem.* **95**, 8118 (1991).

¹³H.-P. Neitzke and R. Terlutter, *Phys. Rev. B* **25**, 1931 (1992).

¹⁴A. J. Saleh and A. J. McCaffery, *J. Chem. Soc., Faraday Trans.* **89**, 3217 (1993).

¹⁵M. J. Weida and D. J. Nesbitt, *J. Chem. Phys.* **100**, 6372 (1994).

¹⁶V. Aquilanti, D. Ascenzi, D. Cappelletti, and F. Pirani, *J. Phys. Chem.* **99**, 13620 (1995).

¹⁷E. B. Anthony, W. Schade, M. J. Bastian, V. M. Bierbaum, and S. R.

- Leone, J. Chem. Phys. **106**, 5413 (1997); E. B. Anthony, Ph.D. thesis, University of Colorado, Boulder, Colorado, 1998.
- ¹⁸S. Harich and A. M. Wodtke, J. Chem. Phys. **107**, 5983 (1997).
- ¹⁹V. Aquilanti, D. Ascenzi, D. Cappelletti, and F. Pirani, J. Phys. Chem. **103**, 4424 (1999).
- ²⁰V. Aquilanti, D. Ascenzi, D. Cappelletti, M. De Castro, and F. Pirani, J. Chem. Phys. **109**, 3839 (1998).
- ²¹V. Aquilanti, D. Ascenzi, M. Bartolomei, D. Cappelletti, S. Cavalli, M. de Castro Víttores, and F. Pirani, Phys. Rev. Lett. **82**, 69 (1999).
- ²²W. Happer, E. Miron, S. Schaefer, D. Schreiber, W. A. van Wijngaarden, and X. Zeng, Phys. Rev. A **29**, 3092 (1984).
- ²³R. Altkorn, R. N. Zare, and C. H. Greene, Mol. Phys. **55**, 1 (1985).
- ²⁴The experimental conditions used for supersonic expansions (in particular source pressure, nozzle diameter,...) lead to very low rotational temperatures, i.e., over 95% of oxygen molecules populate spin-rotation levels ($J=0,1,2$) corresponding to $K=1$. See for instance A. Amirav, U. Even, J. Jortner, and L. Kleinman, J. Chem. Phys. **73**, 4217 (1980); J. Mettes, B. Heijmen, J. Reuss, and D. C. Lainè, Chem. Phys. **87**, 1 (1984); A. Gedanken, N. A. Kuebler, M. B. Robin, and D. R. Herrick, *ibid.* **90**, 3981 (1989); T. Matsumoto and K. Kuwata, Chem. Phys. Lett. **171**, 314 (1990).
- ²⁵V. Aquilanti, D. Ascenzi, D. Cappelletti, S. Franceschini, and F. Pirani, Phys. Rev. Lett. **74**, 2929 (1995).
- ²⁶V. Aquilanti, D. Ascenzi, R. Fedeli, and F. P. Pirani, J. Phys. Chem. A **101**, 7648 (1997). Measured anisotropy effects reported in this paper for N_2 were of the same magnitude as previously reported for the scattering of NO, state selected by a hexapolar field and oriented by means of a magnetic field: H. H. W. Thuis, S. Stolte, and J. Reuss, Chem. Phys. **43**, 351 (1979); H. H. W. Thuis, S. Stolte, J. Reuss, J. J. H. van den Biesen, and C. J. N. van den Meijdenberg, *ibid.* **52**, 211 (1980).
- ²⁷The focus on v as the appropriate quantization axis to describe the polarization arises from the physics of the phenomenon under study—alignment by collision—and from its suitability for perspective applications of scattering experiments with polarized molecules.
- ²⁸The velocity slip is the difference between the flow speeds of the seeded molecules and of the carrier gas: along the beam axis it coincides with the CM collision velocity.
- ²⁹D. P. Pulmann, B. Friedrich, and D. R. Herschbach, J. Phys. Chem. **99**, 7407 (1995).
- ³⁰D. A. Coombe, B. C. Sanctuary, and R. F. Snider, J. Chem. Phys. **63**, 3015 (1975).
- ³¹M. H. Alexander, P. J. Dagdigian, and A. E. DePristo, J. Chem. Phys. **66**, 59 (1977).
- ³²L. Monchick, J. Chem. Phys. **75**, 3377 (1981).
- ³³M. H. Alexander and S. L. Davis, J. Chem. Phys. **78**, 6754 (1983).
- ³⁴A. J. McCaffery, M. J. Proctor, E. A. Seddom, and A. Ticktin, Chem. Phys. Lett. **132**, 185 (1986).
- ³⁵A. J. McCaffery, in *Status and Future Developments in the Study of Transport Properties*, edited by W. Wakeham, A. S. Dickinson, and F. R. McCourt (Kluwer, Dordrecht, 1992), p. 175.
- ³⁶A. M. Arthurs and A. Dalgarno, Proc. R. Soc. London, Ser. A **256**, 540 (1960).
- ³⁷J. Reuss and S. Stolte, Physica (Amsterdam) **42**, 111 (1969).
- ³⁸H. Meyer and S. R. Leone, Mol. Phys. **63**, 705 (1988).
- ³⁹W.-K. Liu and A. S. Dickinson, Mol. Phys. **71**, 1117 (1990).
- ⁴⁰B. Follmeg, P. Rosmus, and H. J. Werner, J. Chem. Phys. **93**, 4687 (1990).
- ⁴¹S. Miller, J. Tennyson, B. Follmeg, P. Rosmus, and H. J. Werner, J. Chem. Phys. **89**, 2178 (1988).
- ⁴²B. Follmeg, H. J. Werner, and P. Rosmus, J. Chem. Phys. **95**, 979 (1991).
- ⁴³L. Beneventi, P. Casavecchia, and G. G. Volpi, J. Chem. Phys. **85**, 7011 (1986).
- ⁴⁴M. H. Alexander, J. Chem. Phys. **67**, 2703 (1977); M. H. Alexander, Chem. Phys. **27**, 229 (1978).
- ⁴⁵J. M. Hutson, S. Green MOLSCAT computer code, distributed by Collaborative Computational Project No. 6 of the Engineering and Physical Sciences Research Council (UK), available on the WEB at <http://www.giss.nasa.gov/molscat/>. The calculations have been performed on an ALPHA AXP 2100 computer available at the Universidad Complutense de Madrid. See also M. De Castro Víttores, *Tesi di Dottorato*, Università di Perugia (1998).
- ⁴⁶The relations between angles in the CM and LAB systems can be visualized by means of the Newton diagrams (see later Figs. 9 and 10): for comparisons between calculated angular distributions and observed quantities, note that angular ranges near the backward direction ($\Theta = \pi$) correspond to a narrow cone in the forward direction of the supersonic expansion.
- ⁴⁷V. Aquilanti, D. Ascenzi, D. Cappelletti, M. de Castro Víttores, and F. Pirani, in *Advances in Molecular Beam Research and Applications*, edited by R. Campargue (Springer-Verlag, Berlin, in press).
- ⁴⁸Quantum mechanical *low* and *high helicities* correspond classically to near *edge-on* and near *broad-side* configurations, respectively.
- ⁴⁹From the relationship between the orbital angular momentum quantum number l and the classical impact parameter b , $\mu vb = \hbar \cdot (l + 1/2)$, we can classify the *large* and *small b* ranges as limited by $b \approx 0.3$ nm, corresponding to the O_2 -He van der Waals radius. For l , we obtain $l \approx 3-20$ for the typical velocity slip range $200-1200$ ms^{-1} and μ , the reduced mass of the O_2 -He system.
- ⁵⁰For benzene molecule, see Sec. V. Aquilanti, D. Ascenzi, D. Cappelletti, D. Di Tommaso, and F. Pirani, MOLEC XII, *European Conference on Dynamics of Molecular Collisions*, 6-11 September 1998, Bristol, UK.